95642

UMTRI-2001-12

QUANTITATIVE EVALUATION OF SEAT SURFACE PRESSURE DISTRIBUTIONS, BODY WEIGHT DISTRIBUTIONS, AND POSTURES OBTAINED WITH HUMAN SURROGATES

Matthew P. Reed
Michelle M. Lehto

University of Michigan Transportation Research Institute

Biosciences Division

April 2001

UMTRI The University of Michigan Transportation Research Institute

QUANTITATIVE EVALUATION OF SEAT SURFACE PRESSURE DISTRIBUTIONS, BODY WEIGHT DISTRIBUTIONS, AND POSTURES OBTAINED WITH HUMAN SURROGATES

Final Report

by

Matthew P. Reed
Michelle M. Lehto

Biosciences Division
University of Michigan Transportation Research Institute

UMTRI-2001-12

Submitted to:

Alliance of Automobile Manufacturers

April 2001

Technical Report Documentation Page

1. Report No.	2. Government Accession No.	3. Recipient's Catalog No.
UMTRI-2001-12		
4. Title and Subtitle Quantitative Evaluation of Seat Surface Pressure Distributions, Body Weight Distributions, and Postures Obtained with Human Surrogates		5. Report Date April 2001 6. Performing Organization Code
7. Author(s) Reed, M.P., Lehto, M.M.		8. Performing Organization Report No. UMTRI-2001-12
9. Performing Organization Name and Address The University of Michigan Transportation Research Institute 2901 Baxter Road Ann Arbor, Michigan 48109-2150 U.S.A.		10. Work Unit no. (TRAIS) 11. Contract or Grant No.
12. Sponsoring Agency Name and Address Alliance of Automobile Manufacturers		13. Type of Report and Period Covered 14. Sponsoring Agency Code
15. Supplementary Notes		

16. Abstract

Seat surface pressure distributions of Hybrid III dummies and Occupant Classification Anthropomorphic Test Devices (OCATDs) representing small adult women and six-year-old children were recorded in a range of postures on two test seats. Support forces under the feet and surrogate postures were also measured. The pressure distribution data were analyzed using quantitative metrics developed in previous testing with human subjects. Both the Hybrid IIIs and OCATDs were found to be reasonably representative of similarly sized humans, but the OCATD6 performance was slightly better than the six-year-old Hybrid III on some parameters. In repeated trials, the coefficient of variance of pressure distribution parameters for all surrogates was generally less than five percent, compared with a 30 percent difference in target values between the child and adult surrogates. Positioning repeatability was better for the child surrogates than for the adult surrogates. The pressure distribution and foot support forces produced by the adult surrogates are strongly influenced by foot position. The data illustrate some of the challenges faced by seat-based occupant classification systems and suggest that pressure-distribution-related parameters may be a useful complement to seat weight sensor data.

17. Key Words		18. Distribution Statement	
Airbags, Pressure Distribution, Occupant Characterization, Anthropometry		Unlimited	
19. Security Classification (of this report)	20. Security Classification (of this page)	21. No. of Pages	22. Price
None	None	30	

CONTENTS

ACKNOWLEDGEMENTS

The authors acknowledge the valuable assistance of Mike Carlson from First Technology Safety Systems, Inc. Thanks also to Paul Starck of Ford Motor Company who provided the six-year-old Hybrid III dummy used in testing.

LIST OF FIGURES

LIST OF TABLES

ABSTRACT

Seat surface pressure distributions of Hybrid III dummies and Occupant Classification Anthropomorphic Test Devices (OCATDs) representing small adult women and six-year-old children were recorded in a range of postures on two test seats. Support forces under the feet and surrogate postures were also measured. The pressure distribution data were analyzed using quantitative metrics developed in previous testing with human subjects. Both the Hybrid IIIs and OCATDs were found to be reasonably representative of similarly sized humans, but the OCATD6 performance was slightly better than the six-year-old Hybrid III on some parameters. In repeated trials, the coefficient of variance of pressure distribution parameters for all surrogates was generally less than five percent, compared with a 30 percent difference in target values between the child and adult surrogates. Positioning repeatability was better for the child surrogates than for the adult surrogates. The pressure distribution and foot support forces produced by the adult surrogates are strongly influenced by foot position. The data illustrate some of the challenges faced by seat-based occupant classification systems and suggest that pressure-distribution-related parameters may be a useful complement to seat weight sensor data.

1.0 INTRODUCTION

Federal Motor Vehicle Safety Standard (FMVSS) 208 mandates passenger airbag systems for frontal impacts that either suppress deployment when a child is present or deploy in a non-injurious manner, but deploy normally when a small adult woman is present. The standard specifies that suppression systems may be tested using either Hybrid III dummies or human volunteers who approximately match the body sizes of the small adult female and six-year-old Hybrid III dummies.

The development of suppression systems, and advanced airbag systems in general, has been hampered by a lack of suitable surrogates for human occupants. In particular, the Hybrid III dummies are difficult to position and may not appear human-like to sensor systems used for occupant classification. Testing with human volunteers is time-consuming and large numbers of subjects are required.

The Alliance of Automobile Manufacturers has supported a research and development program to create a new family of surrogates specifically designed for use in the development of occupant classification systems for advanced airbags. UMTRI has provided anthropometric and performance specifications to First Technology Safety Systems (FTSS), who have developed new Occupant Classification Anthropomorphic Test Devices (OCATDs) representing a small adult woman and a six-year-old child (Reed et al. 2000; 2001).

In a previous study, the seat surface pressure distributions of 68 children and small women were measured in a range of seats and postures (Reed et al. 2000). These data were used to develop quantitative descriptions of typical pressure distributions for the two body sizes specified in FMVSS 208 for suppress system testing. The pressure distributions produced by the small adult female OCATD and six-year-old OCATD (OCATD5 and OCATD6, respectively) were demonstrated to be quantitatively representative of the pressure distributions of similarly sized people.

In the current study, seat surface pressure distributions produced by the small adult female and six-year-old Hybrid III dummies were measured and compared to those produced by human occupants and the OCATDs (Reed et al. 2000). The quantitative comparison was made using pressure-distribution parameters that were demonstrated in the previous research to have value for occupant classification. In the current testing, the positions of the surrogates were recorded using a coordinate measurement machine to quantify the repeatability of the installation procedures. In addition, the support forces under the feet of the surrogate were recorded to evaluate the extent to which the weight borne by the seat varies with posture.

2.0 METHODS

2.1 Surrogates

Testing was conducted with four surrogates, shown in Figure 1:

- Hybrid III small adult female dummy (SFH3),
- Hybrid III six-year-old dummy (6YOH3),
- OCATD5, representing a small adult female, and
- OCATD6, representing a six-year-old child.

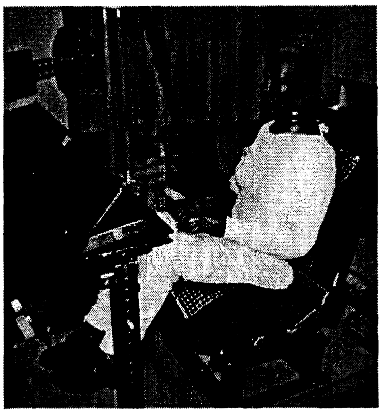

Small Female Hybrid III

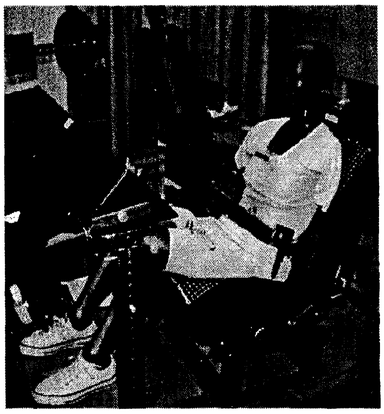

OCATD5

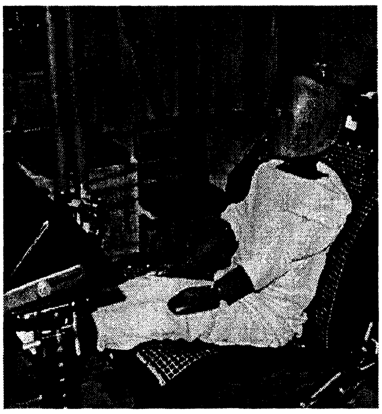

Six-Year-Old Hybrid III

OCATD6

Figure 1. Surrogates used in testing.

2.2 Seats

Testing was conducted using two seats, shown in Figure 2, that were selected from the five used in the previous study. Seat 0 is constructed of soft foam and provides pressure distribution measurements that are free of artifacts caused by seat contouring and seams. The OCATD performance specifications were developed from human subject data obtained on seat 0. Seat 4 is a firm seat with minimal contouring that provides a contrast to the soft foam of seat 0.

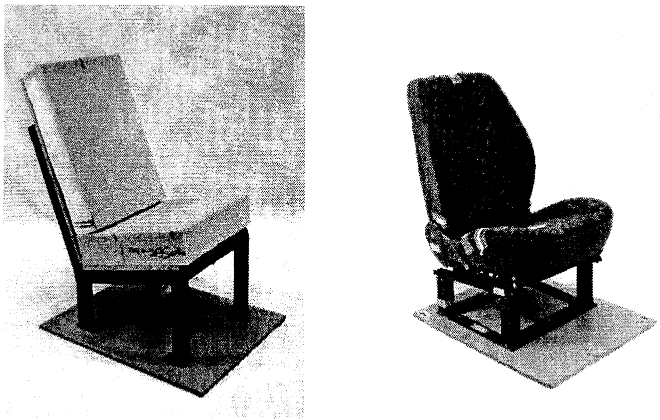

Seat 0 Seat 4

Figure 2. Test seats. Numbering is consistent with previous study (Reed et al. 2000).

2.3 Pressure Distribution Measurement System

Pressure distributions were measured with the system used in the previous study (Reed et al. 2000). The Xsensor system is comprised of two pressure-sensing mats and a computer interface. Figure 3 shows the Xsensor system applied to a seat. The mats are about 3 mm thick and can be flexed on multiple axes so that they conform easily to the deflected seat contour. Each mat contains 1296 capacitative sensors arranged in a 36 x 36 array. Each sensor is square, measuring 12.5 mm (0.5 inch) on each side. The sensors were sampled at 10-second intervals during data collection. For testing, the sensing mats were affixed to the seat using double-sided cloth adhesive tape. Clips were placed on each mat to mark the seat H-point location, as measured by the SAE J826 H-point machine.

The Xsensor system was calibrated weekly during testing by placing each mat in a flat chamber with a pneumatic bladder. Inflating the bladder applies a uniform pressure on the mat. The sensor responses to a series of known pressures are stored in a calibration file. As an additional calibration check, a pilot calibration is performed after each subject's trials on a seat. The mats are laid on a rigid, flat surface, and a pressure is applied over a circular area using a known weight. The resulting calibration data are used to adjust the measured values to account for drift in the values during testing. Typical corrections are less than ten percent. The previous report includes documentation of the system performance (Reed et al. 2000).

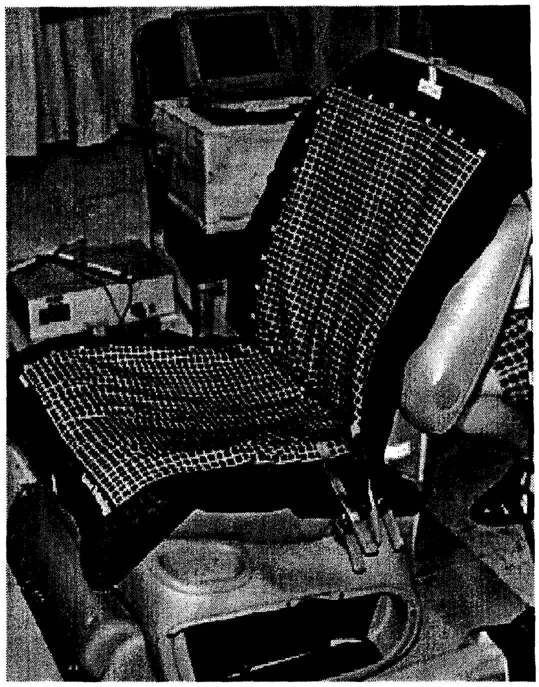

Figure 3. Xsensor pressure distribution measurement system on a test seat, showing clips applied to mark H-point location.

2.4 Force Platform

A six-axis force platform was mounted on the test platform in front of the seat. The forces exerted on the platform by the surrogates' feet were recorded in each test condition. Figure 4 shows the force platform location.

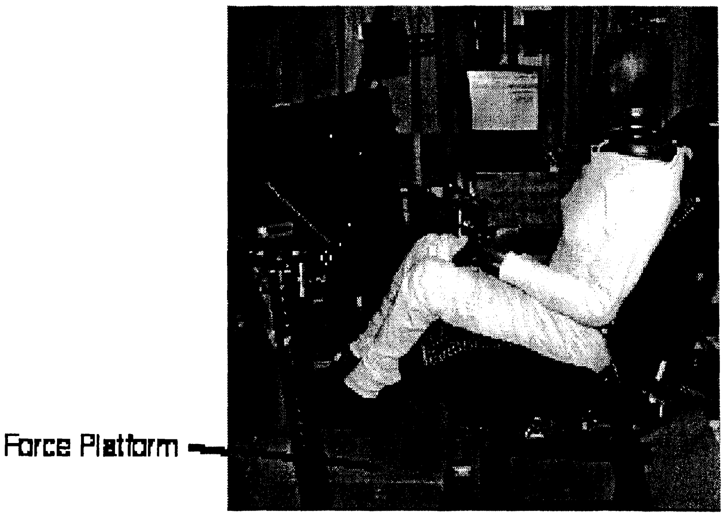

Figure 4. Force platform used to record resting foot forces.

2.5 Posture and Position Data

The location and posture of the surrogate was measured in the normal position by digitizing the locations of landmarks and reference points with a FARO arm. Table 1 lists the points digitized on each surrogate.

Table 1
Landmarks and Reference Points

Left H-Point	Infraorbitale
Right H-Point	Corner of Eye
Hip Bolt	C7
Knee Bolt	Top of Sternum
Top of Knee	Bottom of Sternum
Ankle Bolt	Left ASIS
Heel Contact	Right ASIS
Ball of Foot	Pubic Symphysis
Top of Head	Shoulder Bolt*
Head CG	Elbow Bolt*
Occiput	Center of Wrist*
Glabella	

* Not available on OCATDs.

2.6 Test Postures

Each surrogate was tested in a number of different postures. Table 2 lists the postures and the surrogates with which they were used. The normal position was repeated five times with each surrogate. The Normal-90 and Foot-Position conditions were repeated five times with each of the adult surrogates. Reclined postures were tested only in seat 4, because the seatback on seat 0 did not recline.

Table 2
Test Postures

Posture	Definition	Surrogates	Illustration
Normal	Surrogate is placed in a normal passenger posture, sagittally symmetric, looking straight ahead, with heels resting on the floor and moved maximally forward. The hands rest on the thighs. Seat back angle (SAE L40) set to 23 degrees. The child surrogates were placed full-rear on the seat cushion. The feet of the child surrogates did not reach the floor.	SFH3 6YOH3 OCATD5 OCATD6	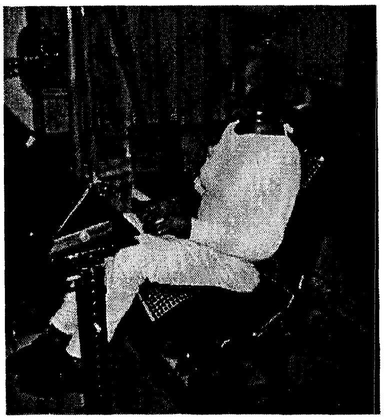
Normal 90	Normal posture, but with feet positioned so that knees are flexed 90 degrees	SFH3 OCATD5	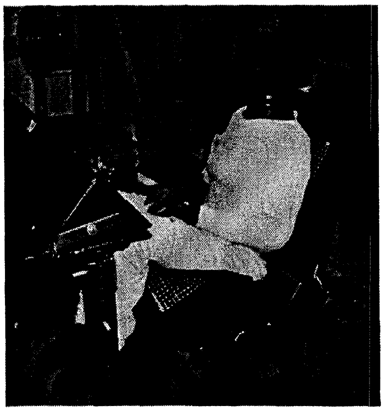
Foot Positions	Three foot positions evenly spaced between the foot positions obtained in the Normal and Normal 90.	SFH3 OCATD5	
Knees Up	With feet on the front edge of the seat, arms wrapped around legs.	6YOH3 OCATD6	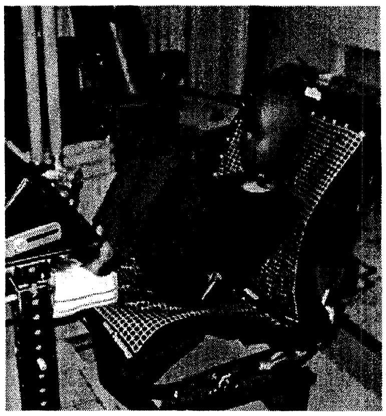

Table 2
Test Postures (continued)

Forward	From normal posture, leaning forward to touch target.	SFH3 6YOH3 OCATD5 OCATD6	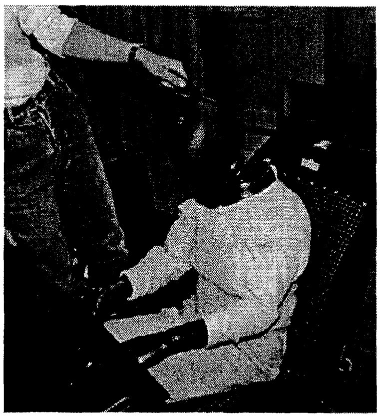
Lean	Leaning to right onto armrest from normal posture.	SFH3 6YOH3 OCATD5 OCATD6	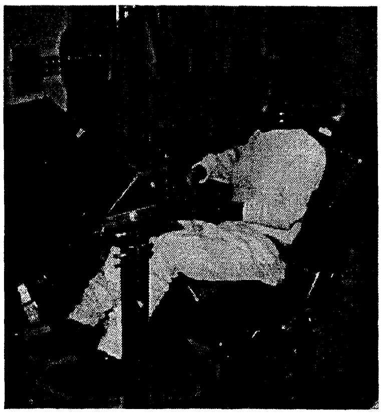
Legs Crossed	Crossing right leg over left at knee from normal posture.	OCATD5 OCATD6	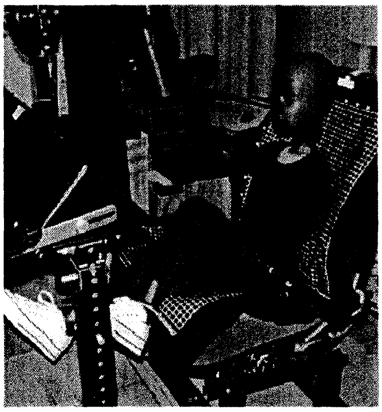
Slouched	Slide hips forward approximately 150 mm from normal posture.	SFH3 6YOH3 OCATD5 OCATD6	

Table 2
Test Postures (continued)

Normal Recline (30 degrees)*	Normal posture with a 30-degree seatback angle (SAE L40)	SFH3 6YOH3 OCATD5 OCATD6	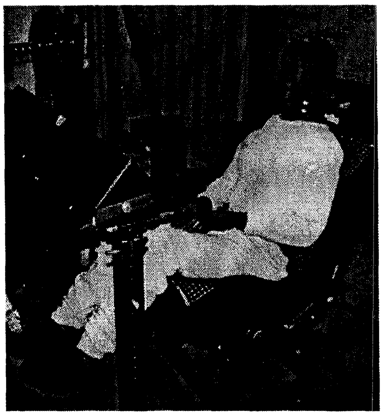
Extreme Recline (45 degrees)*	Normal posture with a 45-degree seatback angle (SAE L40)	SFH3 6YOH3 OCATD5 OCATD6	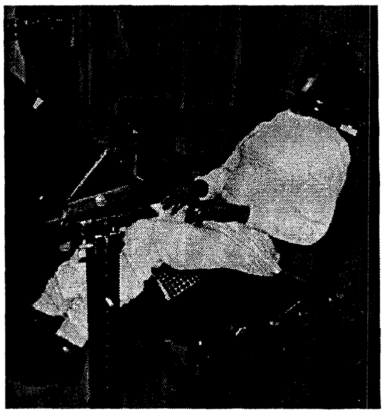
Normal Recline 90 (30 degrees) *	Normal posture with a 30-degree seatback angle (SAE L40) with knees flexed 90 degrees	SFH3 OCATD5	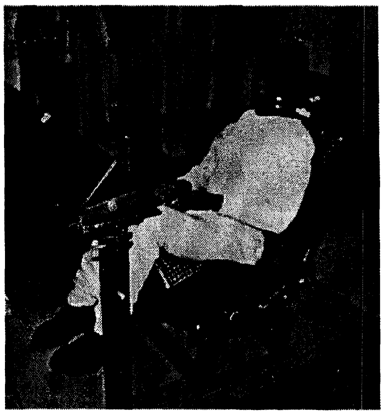
Extreme Recline 90 (45 degrees)*	Normal posture with a 45-degree seatback angle (SAE L40) with knees flexed 90 degrees	SFH3 OCATD5	

* Reclined conditions tested in Seat 4 only.

Table 2
Test Postures (continued)

Kneel Backwards	Kneeling on seat facing backward.	6YOH3 OCATD6	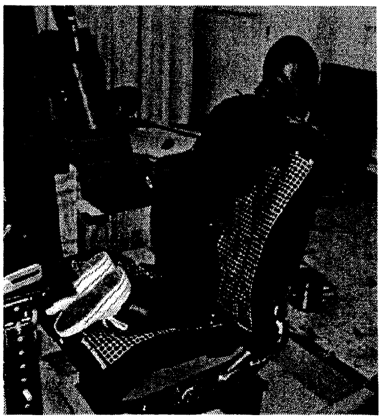
Scoot	Sitting on front of seat with knees flexed 90 degrees	6YOH3 OCATD6	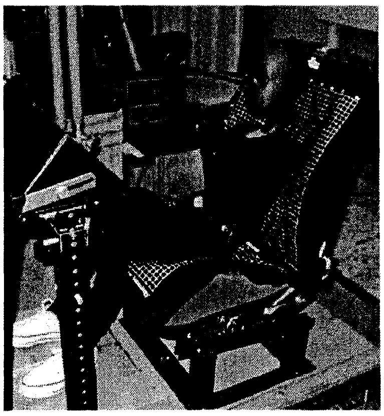

3.0 RESULTS

3.1 Qualitative Evaluation of Surrogate Pressure Distributions

Figure 5 shows a typical pressure distribution from the seat cushion pad, with several features labeled and with pressure levels displayed with different colors . In this report, all pressure distribution illustrations are from the seat cushion and are best viewed in color. The front of the seat cushion is at the top of each image. The isolated pressure peak at the left side of the image is produced by a clamp applied to mark the seat H-point location. The pressure distribution image is a two-dimensional representation of the pressure on a three-dimensional, contoured interface. All of the pressure distribution images in this report present the data in a scaled, relative-pressure format. In each image, the highest pressures are represented in red and the lowest in dark blue. Areas where the pressure was less than 5 mmHg are shown in black. Because the pressure axis is scaled, a red pressure area in one image may represent a different pressure than the red areas of another image. This approach provides a good illustration of the distribution of pressures, independent of their peak values.

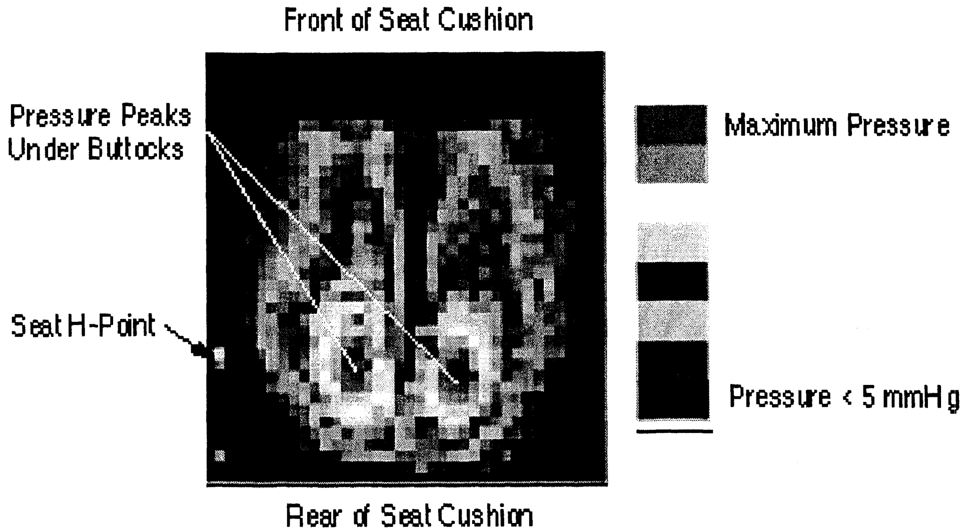

Figure 5. Typical pressure distribution in a normal posture, with various features labeled.

3.1.1 Posture Effects

Table 3 shows the seat cushion pressure distributions from the adult surrogates in selected postures. Table 4 compares the pressure distributions from the child surrogates. There are substantial qualitative differences between the Hybrid III and OCATD pressure distributions. The SFH3 pressure distribution is wider and more angular in the buttock area, and shows distinct artifacts caused by flesh seams in the thighs. The ischial pressure peaks under the buttocks are more widely spaced for the SFH3 than for the OCATD and the human.

The 6YOH3 also shows artifacts due to flesh seams. The flatter 6YOH3 buttock surface appears to produce a more uniform (and hence unrealistic) pressure distribution than the OCATD6.

3.1.2 Seat Effects

Tables 5 and 6 show the substantial effects of seat foam stiffness on the pressure distributions produced by humans and the surrogates. The stiffer foam on seat 4 accentuates the differences between the Hybrid IIIs and the OCATDs. With the stiffer seat foam, the Hybrid IIIs produce essentially flat pressure distributions in the normal posture, without well-defined ischial peaks. The OCATD flesh, which is softer and more contoured than the Hybrid IIIs, produces apparently more human-like pressure contours on the firm seat, particularly in the buttock area. There are still visible differences between the OCATD and the human pressure distributions on the firm seat. The human buttock tissue in the buttock area is softer than that of the OCATDs, producing smoother pressure gradients than are obtained with the OCATD. One consequence is that the OCATD pressure peaks appear flatter than those obtained with humans on firm seats. However, the buttock contour of the OCATDs improves the pressure distribution on both soft and firm seats relative to the Hybrid IIIs.

Table 3
Pressure Distributions for Adult Surrogates on Seat 0

Posture	Small Adult Female Hybrid III	OCATD5	Typical Small Woman
Normal 	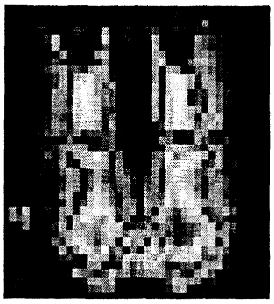	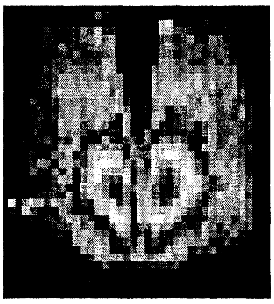	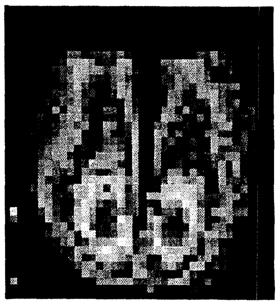
Normal 90 	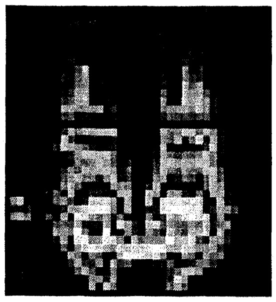	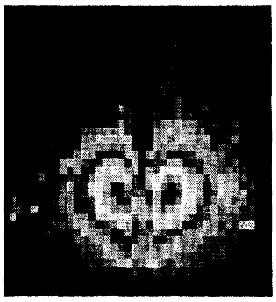	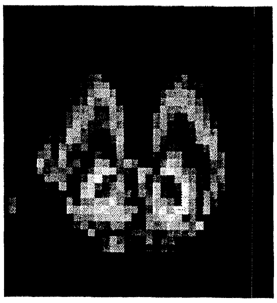
Lean 	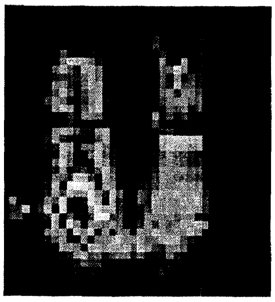	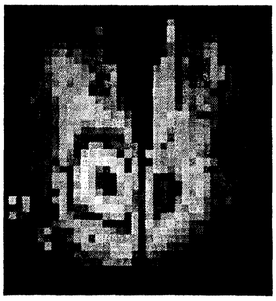	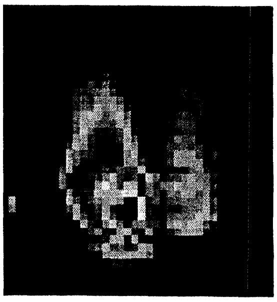
Forward 	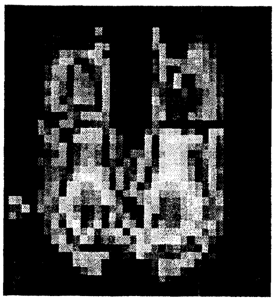	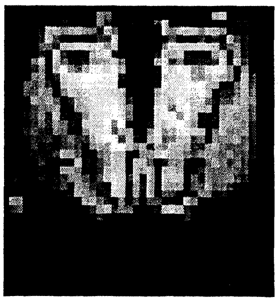	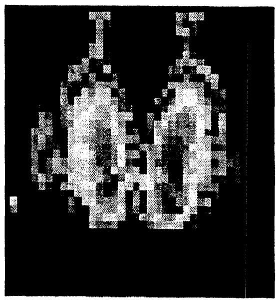

Table 4
Pressure Distributions for Child Surrogates on Seat 0

Posture	Six-Year-Old Hybrid III	OCATD6	Typical Six-Year-Old Child
Normal 	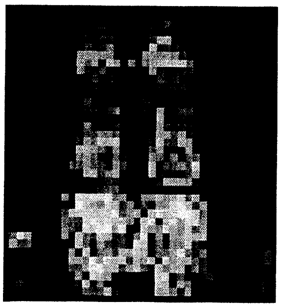	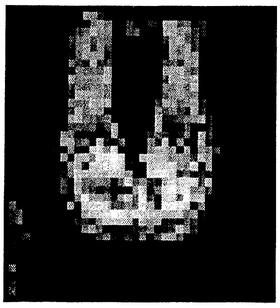	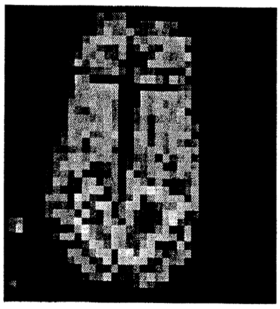
Knees Up 	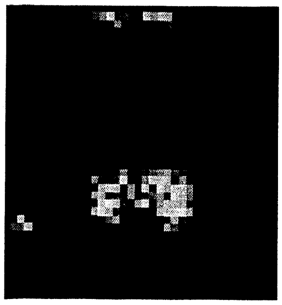	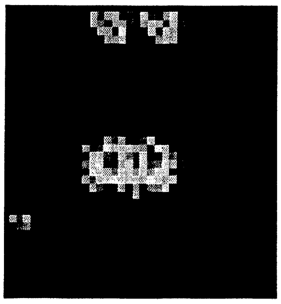	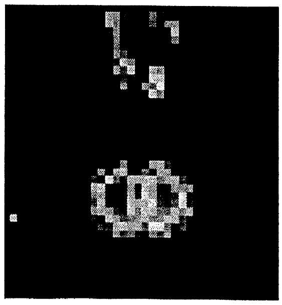
Lean 	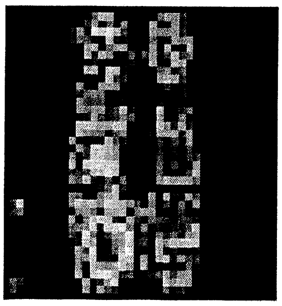	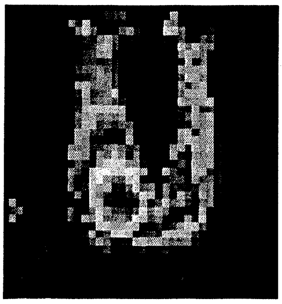	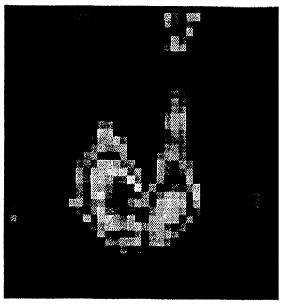
Forward 	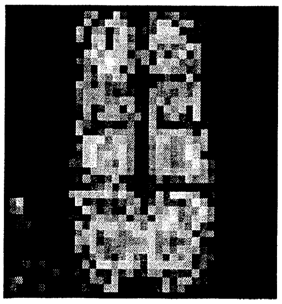	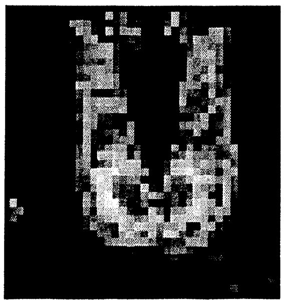	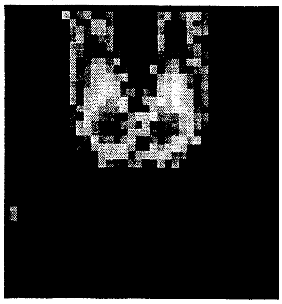

Table 5
Comparison of Pressure Distributions in Seat 0 and Seat 4 in the Normal Posture for Adult Surrogates

Surrogate	Seat 0	Seat 4
	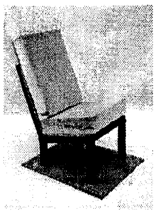	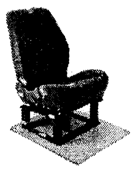
Small Female Hybrid III 		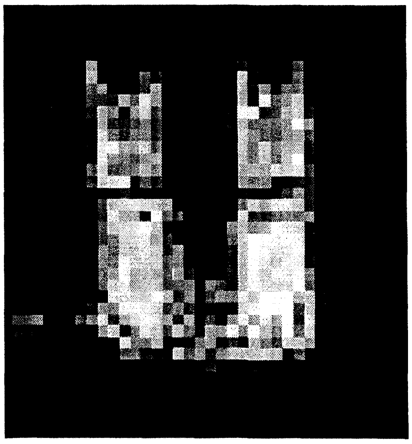
OCATD5 	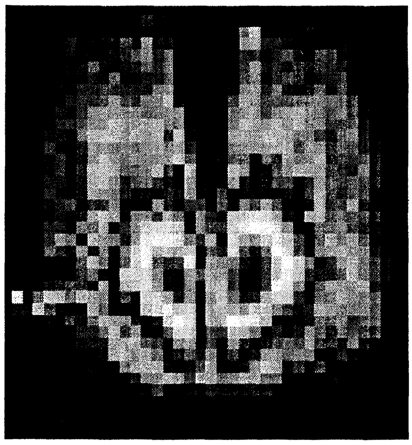	
Typical Small Woman 	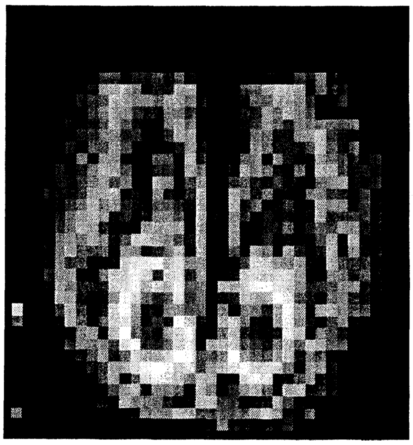	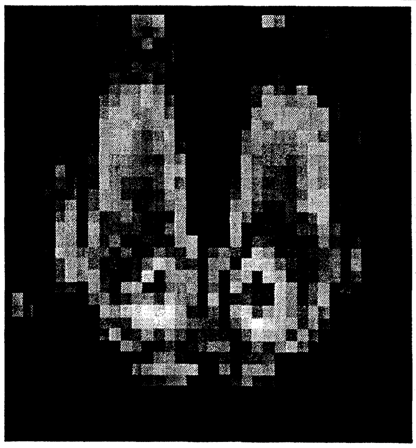

Table 6
Comparison of Pressure Distributions in Seat 0 and Seat 4 in the Normal Posture for Child Surrogates

Surrogate	Seat 0	Seat 4
	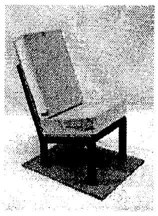	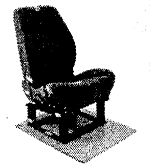
Six-Year-Old Hybrid III 	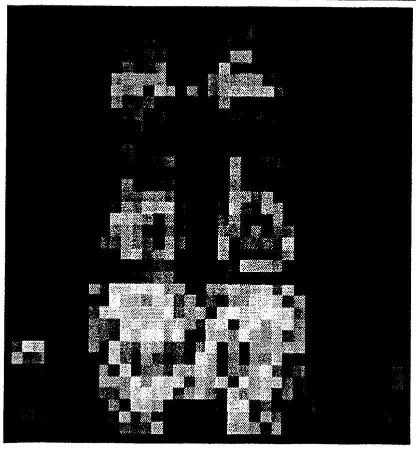	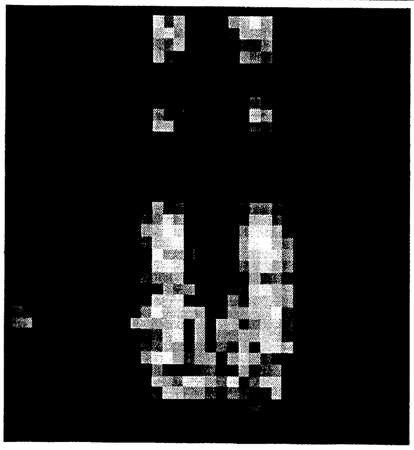
OCATD6 	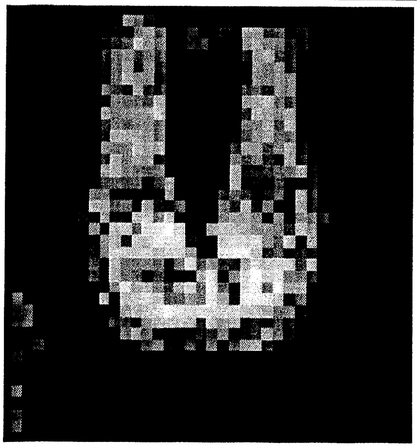	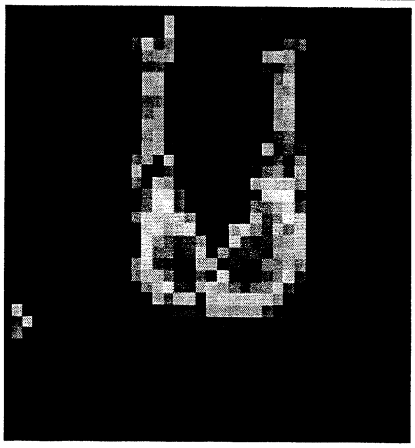
Typical Six-Year-Old Child 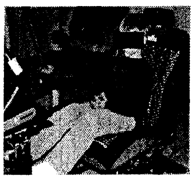	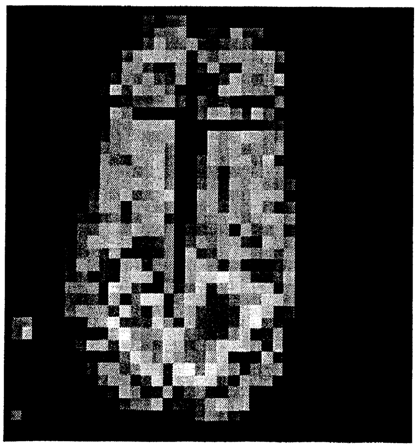	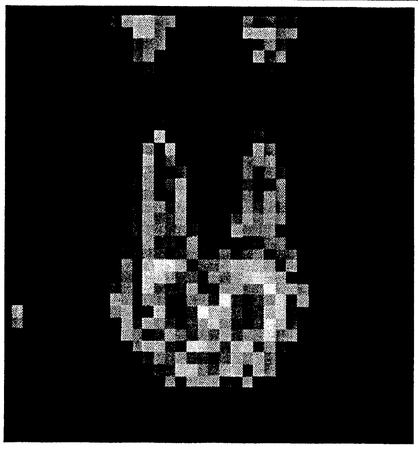

3.2 Quantitative Evaluation of Surrogate Pressure Distributions

3.2.1 Parameter Calculation

In the previous study with human subjects, a large number of parameters were calculated from the seat surface pressure data in an effort to identify characteristics of the pressure distribution that were useful for occupant classification. Results for a subset of these parameters were reported. The occupant-classification value of each parameter was assessed by predicting occupant body mass from the parameter values using data from 68 people. The best prediction was obtained with width- and area-related measures, along with pseudoweight. Pseudoweight was obtained by summing the pressure measured by each sensor and multiplying by the sensor area. Table 7 lists the definitions for the 10 parameters that provided the best prediction of occupant body mass in the previous study. These parameters are used in the analyses that follow.

Table 7
Pressure Distribution Parameter Definitions

Parameter	Definition (units)
PeakRowWidthP10	Maximum lateral distance separating sensors reading at or above 10 mmHg in the lateral row containing the highest pressure peak (sensor units)
CentroidRowWidthQ20	Maximum lateral distance separating sensors reading at or above the 20th-percentile pressure in the lateral row containing the pressure distribution centroid (sensor units)
PseudoWeightLb	Sum of the product of sensor pressure and sensor area (lb)
CentroidRowWidthP10	Maximum lateral distance separating sensors reading at or above the 10 mmHg in the lateral row containing the pressure distribution centroid (sensor units)
CentroidRowWidthQ10	Maximum lateral distance separating sensors reading at or above the 10th-percentile pressure in the lateral row containing the pressure distribution centroid
PeakRowWidthQ10	Maximum lateral distance separating sensors reading at or above the 10th-percentile pressure in the lateral row containing the highest pressure peak (sensor units)
AreaP10	Area of the pressure distribution exceeding 10 mmHg (cm^2)
AreaQ20	Area of the pressure distribution exceeding the 20th percentile of pressure (cm^2)
AreaQ10	Area of the pressure distribution exceeding the 10th percentile of pressure (cm^2)
PeakRowWidthQ20	Maximum lateral distance separating sensors reading at or above the 20th-percentile pressure in the lateral row containing the highest pressure peak (sensor units)

* Each sensor unit is 0.5 inch (12.7 mm).

Target values for each parameter were established for the OCATD5 and OCATD6, using regression functions predicting the parameter value from body mass. Substituting the OCATD5 and OCATD6 masses produced target parameter values for each surrogate. Because of anthropometric and postural variability, each of these regression analyses yielded a residual variance estimate that describes the distribution of the parameter value expected for a population of occupants who match the surrogate's body weight. Table 8 lists the results of the regression analyses from the previous study with human volunteers, along with the OCATD5 and OCATD6 targets.

Table 8
Regression Results Predicting Occupant Body Mass from Parameter Values (Reed et al. 2000)

Parameter	R^2	Intercept *	Slope *	RMSE *	Intercept †	Slope †	RMSE †	OCATD6 Target**	OCATD5 Target**
PeakRowWidthP10	0.88	-88.2	6.95	7.7	14.1	0.13	1.04	20.6	27.7
CentroidRowWidthQ20	0.86	-69.1	6.31	8.3	12.7	0.14	1.21	19.7	27.4
PseudoWeightLb	0.85	-7.6	1.05	8.6	18.5	0.80	7.52	59.9	105.3
CentroidRowWidthP10	0.85	-91.5	6.91	8.6	15.0	0.12	1.15	21.3	28.2
CentroidRowWidthQ10	0.84	-78.7	6.49	8.8	14.1	0.13	1.25	20.7	28.0
PeakRowWidthQ10	0.84	-72.9	6.48	8.9	13.2	0.13	1.26	19.9	27.1
AreaP10	0.81	-38.3	0.11	9.5	475.7	7.32	77.18	852.9	1266.7
AreaQ20	0.79	-38.3	0.13	10.0	422.5	6.17	69.30	740.5	1089.4
AreaQ10	0.79	-37.3	0.11	10.1	472.5	6.92	79.02	829.0	1220.1
PeakRowWidthQ20	0.78	-60.8	6.21	10.4	12.6	0.13	1.48	19.0	26.1

* Regression predicting body weight as a function of parameter value.
† Regression predicting parameter value as a function of body weight.
** Target values calculated by using OCATD5 and OCATD6 target weights of 51.5 and 108 lb, respectively.

In the current study, values for the same parameters were calculated for each seat surface pressure distribution. As in the previous analysis, only data from the seat cushion were used. One conclusion from the previous study was that the leg position of the surrogate influences the correspondence with the human subject data on some parameters. In particular, unrealistic values on area-related parameters can be obtained if the surrogates' legs are positioned in a manner substantially different from the postures used by the human subjects. As was done with the OCATD5 evaluations in the previous study, the adult surrogates in the current study were tested in the normal posture with five different foot positions (see Table 2).

3.2.2 Comparisons with Human-Derived Targets

Tables 9 and 10 compare the measured parameter values for the SFH3 and OCATD5 to the human-derived targets. The tables show the target values along with the RMSE for each parameter from Table 8. Data for five foot positions are shown, averaged across five trials in each position. FP5 is the Normal posture from Table 2 and FP1 is the Normal-90 posture. FP2, FP3, and FP4 are obtained with the feet positioned at even fore-aft increments between the full-forward foot position in the normal posture and the rearward position obtained with the knees flexed 90 degrees. The measured values are expressed with respect to the targets as multiples of the RMSE. Values close to zero indicate that the surrogate matched the target very closely. Absolute values less than 1 indicate that surrogate was within one standard deviation of mean value expected for a population of people who match the surrrogate's body mass.

The tables demonstrate the manner in which some parameters are affected by foot position. For example, the SFH3 area parameters are well below the targets when the knees are up, but meet the targets when the feet are moved forward, engaging the thighs with the seat (shaded column in the table). In contrast, the OCATD5 matches the human data best when the knees are flexed 90 degrees. The difference may be related to shoes -- the OCATD5 was tested with low-heeled shoes, whereas the SFH3 had shoes with higher heels.

Table 9
Comparison with Targets: Small Female Hybrid III on Seat 0 (standard deviation units)

Parameter	Target	RMSE	FP1*	FP2	FP3	FP4	FP5
PeakRowWidthP10	27.7	1.04	-1.06	-1.25	-0.67	-0.87	-0.67
CentroidRowWidthQ20	27.4	1.21	-1.65	-1.16	-1.49	-1.49	-0.99
PseudoWeightLb	105.3	7.52	-1.71	-0.52	0.99	2.26	4.36
CentroidRowWidthP10	28.2	1.15	-1.04	-1.22	-1.04	-0.70	-0.70
CentroidRowWidthQ10	28.0	1.25	-1.12	-1.12	-1.12	-0.96	-0.96
PeakRowWidthQ10	27.1	1.26	-0.71	-0.71	-0.56	-0.71	-0.56
AreaP10	1266.7	77.18	-3.84	-3.24	-2.20	-1.28	-0.08
AreaQ20	1089.4	69.30	-3.27	-2.70	-1.90	-0.83	0.17
AreaQ10	1220.1	79.02	-3.02	-2.64	-1.72	-0.74	0.44
PeakRowWidthQ20	26.1	1.48	-0.20	-0.47	-0.47	-0.20	-0.07

* FPn = Foot Position n, where FP5 is the Normal posture and FP1 is the Normal 90 posture (see Table 2).

Table 10
Comparison with Targets: OCATD5 (Small Adult Female) on Seat 0
(standard deviation units)

Parameter	Target	RMSE	FP1	FP2	FP3	FP4	FP5
PeakRowWidthP10	27.7	1.04	0.29	0.29	0.29	0.29	0.29
CentroidRowWidthQ20	27.4	1.21	0.50	0.50	0.50	0.50	-0.17
PseudoWeightLb	105.3	7.52	0.93	1.32	1.74	2.16	2.12
CentroidRowWidthP10	28.2	1.15	-0.17	-0.17	-0.17	-0.17	-0.17
CentroidRowWidthQ10	28.0	1.25	0.00	0.00	0.00	0.00	0.00
PeakRowWidthQ10	27.1	1.26	0.71	0.71	0.71	0.71	0.71
AreaP10	1266.7	77.18	0.74	1.25	1.74	2.15	2.43
AreaQ20	1089.4	69.30	0.69	1.27	1.47	1.94	2.10
AreaQ10	1220.1	79.02	0.93	1.10	1.63	1.84	2.17
PeakRowWidthQ20	26.1	1.48	1.28	1.28	1.28	1.15	1.01

* FPn = Foot Position n, where FP5 is the Normal posture and FP1 is the Normal 90 posture (see Table 2).

Table 11 compares the normal-posture performance of the 6YOH3 and OCATD6 with the human targets. Parameter values from five trials with each surrogate were averaged. (Because the six-year-old surrogates' feet did not reach the floor in the normal posture, the range of foot positions used with the adult surrogates was not needed.)

The OCATD6 performed better than the 6YOH3 relative to the human targets, particularly on width-related parameters. The values in Table 11 suggest that the pressure distribution produced by the 6YOH3 is narrower than is typical for a six-year-old child. On the area measures, the 6YOHII matched the human targets better than the OCATD6. As with the adult surrogates, the area measures are very sensitive to leg position. With the child surrogates, the extent to which the knees are straightened and the manner in which the back of the calves interact with the seat cushion affects the area measures substantially.

Table 11
Comparison with Targets: Child Surrogates on Seat 0
(standard deviation units)

Parameter	Target	RMSE	6YOH3	OCATD6
PeakRowWidthP10	20.6	1.04	-1.73	-0.26
CentroidRowWidthQ20	19.7	1.21	-1.57	0.52
PseudoWeightLb	59.9	7.52	2.15	-0.06
CentroidRowWidthP10	21.3	1.15	-1.48	0.61
CentroidRowWidthQ10	20.7	1.25	-1.04	0.51
PeakRowWidthQ10	19.9	1.26	-1.03	0.08
AreaP10	852.9	77.18	-0.90	-1.65
AreaQ20	740.5	69.30	-0.32	-1.64
AreaQ10	829.0	79.02	-0.51	-1.60
PeakRowWidthQ20	19.0	1.48	-0.54	0.00

Figures 6 through 9 show the surrogate performance on the pressure distribution parameters graphically. In each figure, the expected distribution of normalized parameter values for humans matching the surrogate body weight is shown on the vertical axis. Horizontal lines indicate the target value (0.0) and standard deviation (RMSE) units. The normalized parameter values from Tables 9 and 10 are plotted for each surrogate. For the adult surrogates, data from the foot position that produced area parameter values best matching the human targets were selected (gray columns from Tables 9 and 10).

The pseudoweight parameter values were dramatically different for the Hybrid IIIs and OCATDs, even though the area and width measures were more comparable. Although no clear explanation has been found for this difference, it may be related to the difference in buttock shape. The OCATDs have a more contoured buttock shape compared with the flatter Hybrid III buttock areas. It should be noted that while pseudoweight was the best overall predictor of occupant body mass in the previous study (see Reed et al. 2000), a true seat weight measure would be unlikely to show the same differences between the OCATDs and Hybrid IIIs.

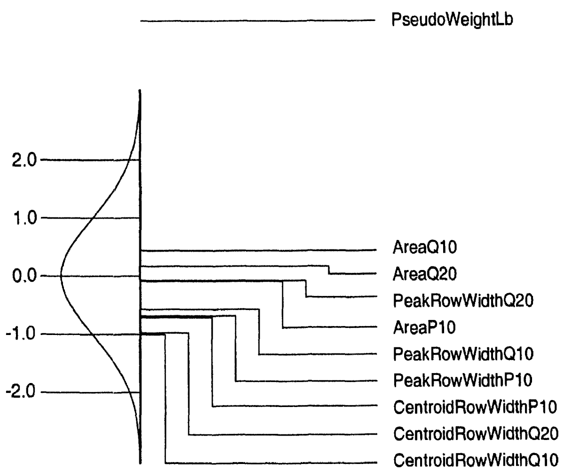

Figure 6. Illustration of **SFH3** performance relative to targets, showing (Observed–Target)/RMSE values from Table 9. Vertical axis shows normalized parameter values in standard deviations relative to human-derived targets.

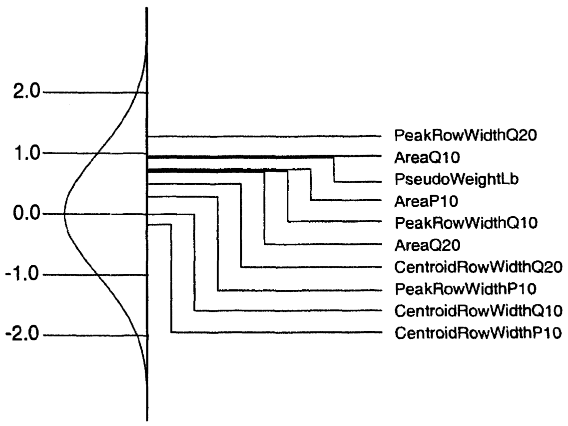

Figure 7. Illustration of **OCATD5** performance relative to targets, showing (Observed–Target)/RMSE values from Table 10. Vertical axis shows normalized parameter values in standard deviations relative to human-derived targets.

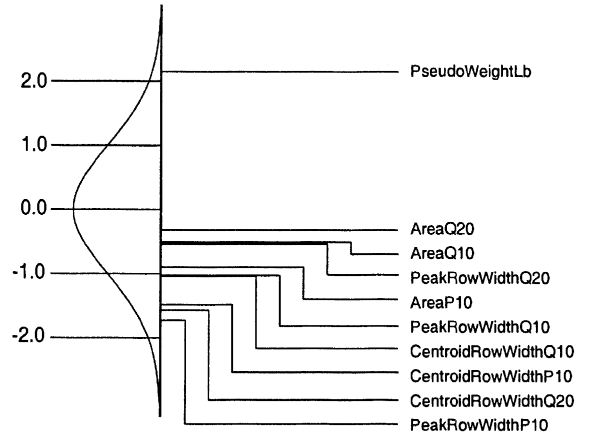

Figure 8. Illustration of **6YOH3** performance relative to targets, showing (Observed–Target)/RMSE values from Table 11. Vertical axis shows normalized parameter values in standard deviations relative to human-derived targets.

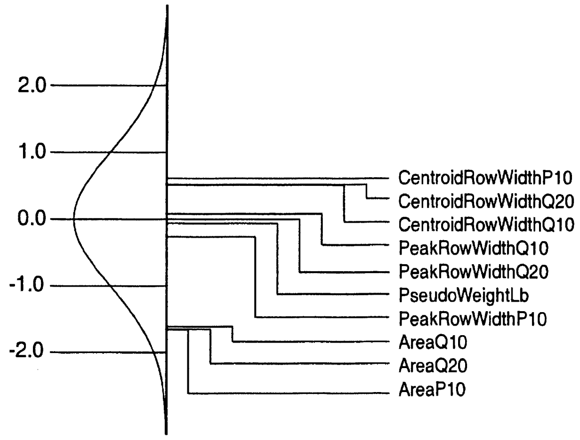

Figure 9. Illustration of **OCATD6** performance relative to targets, showing (Observed–Target)/RMSE values from Table 11. Vertical axis shows normalized parameter values in standard deviations relative to human-derived targets.

3.3 Pressure Parameter Repeatability

Tables 12 and 13 show the means and coefficients of variation for repeated trials in the normal position. (The coefficient of variation is the sample standard deviation divided by the mean, expressed in Tables 12 and 13 as a percentage.) For the adult surrogates, the COV are below five percent. Some COV values are higher for the child surrogates, but are less than ten percent. For all surrogates, the granularity of the sensor spacing affects the COV. For example, the width of the six-year-old surrogates is about 20 sensor units (one sensor unit = 0.5 inch = 12.7 mm). A difference of one sensor unit in the width parameter value, potentially caused by a small lateral shift of the surrogate, represents five percent of the mean. Based on the data in Tables 12 and 13, there do not appear to be substantial differences in pressure distribution measurement precision among the surrogates.

Table 12
Mean and Coefficient of Variation for Five Trials in the Normal Position: Adult Surrogates

Parameter	Target	SFH3		OCATD5	
		Mean	COV*	Mean	COV*
PeakRowWidthP10	27.7	27.0	2.6%	28.0	0.0%
CentroidRowWidthQ20	27.4	26.2	1.6%	27.2	4.0%
PseudoWeightLb	105.3	138.1	3.1%	121.2	4.4%
CentroidRowWidthP10	28.2	27.4	1.9%	28.0	0.0%
CentroidRowWidthQ10	28.0	26.8	1.6%	28.0	0.0%
PeakRowWidthQ10	27.1	26.4	2.0%	28.0	0.0%
AreaP10	1266.7	1260.6	4.2%	1454.2	3.8%
AreaQ20	1089.4	1101.3	4.4%	1235.2	3.0%
AreaQ10	1220.1	1254.5	4.5%	1391.6	2.3%
PeakRowWidthQ20	26.1	26.0	0.0%	27.6	2.1%

*Coefficient of variation is standard deviation divided by mean.

Table 13
Mean and Coefficient of Variation for Five Trials in the Normal Position: Child Surrogates

Parameter	Target	6YOH3		OCATD6	
		Mean	COV*	Mean	COV*
PeakRowWidthP10	20.6	18.8	4.5%	20.3	2.8%
CentroidRowWidthQ20	19.7	17.8	4.7%	20.3	2.8%
PseudoWeightLb	59.9	76.1	5.0%	59.5	9.6%
CentroidRowWidthP10	21.3	19.6	2.8%	22.0	4.5%
CentroidRowWidthQ10	20.7	19.4	2.8%	21.3	2.7%
PeakRowWidthQ10	19.9	18.6	2.9%	20.0	0.0%
AreaP10	852.9	783.2	8.0%	725.8	4.1%
AreaQ20	740.5	718.1	7.1%	626.9	3.4%
AreaQ10	829.0	788.4	8.4%	702.7	5.4%
PeakRowWidthQ20	19.0	18.2	4.6%	19.0	5.3%

*Coefficient of variation is standard deviation divided by mean.

3.4 Surrogate Positioning Repeatability

Table 14 lists the standard deviations of H-point location across five trials with each surrogate in seat 0. The positioning of the larger surrogates was less precise than the smaller surrogates, probably because of the greater difficulty in manipulating the adult surrogates. Vertical variability (Z) was always smaller than fore-aft variability (X). The positioning repeatability for the OCATD6 was surprisingly good. The positioning precision for the OCATD5 is probably improved relative to the SFH3 because of differences in the installation procedure. The SFH3 is initially placed in the seat with the seatback reclined, then the seatback is adjusted to position the ATD torso. In contrast, the OCATD5 is dropped into the seat with the seatback already adjusted to the test position.

Table 14
Standard Deviation of H-point Location for Five Trials
in the Normal Position (mm)

Surrogate	H-Point X	H-Point Z
SFH3	15.0	5.8
OCATD5*	5.9	2.2
6YOH3	9.6	6.1
OCATD6	1.0	0.7

*One anomalous trial with improper execution of the installation procedure was excluded. SD with excluded trial was 20.9 mm.

3.5 Foot Support Forces

The support forces under the surrogates' feet were measured using a force plate. Table 15 shows the vertical reaction force for the adult surrogates in the normal posture with a range of foot positions. As expected, the foot support force decreases when the feet are moved further from the seat, engaging the surrogate's thighs more fully. The fraction of surrogate weight borne by the feet was lower for the OCATD5 than for the SFH3. This may be attributed in part to the taller shoe heels on the SFH3, which yielded less thigh contact with the seat for the SFH3 (see Tables 9 and 10).

The foot forces may also have been affected by the stiffness of theSFH3 hip joint. The pelvis flesh restricts hip joint flexion, producing a non-human-like distribution of support forces when the knees are raised. The resistance from the Hybrid III pelvis flesh may have contributed to the differences in foot support force between the SFH3 and OCATD5.

Table 15
Vertical Foot Support Forces in the Normal Posture
with a Range of Foot Positions (lb)

Foot Position	SFH3			OCATD5		
	Mean	S.D.	% Weight	Mean	S.D.	% Weight
FP1 (Knees Up)	42.0	3.0	39%	18.9	4.7	17%
FP2	33.7	2.8	31%	17.4	2.7	16%
FP3	26.1	4.1	24%	15.4	2.4	14%
FP4	16.0	5.4	15%	12.0	2.1	11%
FP5 (Feet Slid Forward)	10.7	8.9	10%	6.8	2.0	6%

4.0 DISCUSSION

The seat surface pressure distributions produced by the OCATDs are visually more similar to human pressure distributions than those produced by the Hybrid IIIs. The OCATD pressure distributions lack the flesh-seam artifacts observed with the Hybrid IIIs, and the pressure gradients lateral to the ischial tuberosities and under the thighs are more realistic. In general, the flatter buttock areas of the Hybrid IIIs produce flatter pressure distributions than are observed with humans and the OCATDs. However, the quantitative analysis shows that the small adult female Hybrid III is approximately as representative of small adult women as the OCATD5 with respect to the parameters of seat surface pressure distribution that are related to occupant body weight. The previous study demonstrated that the pressure distribution parameters that are most useful for occupant classification are predominantly those related to width and area. On these parameters, the small female Hybrid III is similar to the OCATD5 and to small women, although, as with the OCATD5, the parameter values are sensitive to the surrogate thigh interaction with the seat.

The six-year-old Hybrid III was less representative of six-year-old children than the OCATD6 with respect to pressure distribution parameters. In particular, the 6YOH3 pressure distributions were narrower and smaller in area than those obtained with humans. The OCATD6 pressure distribution matches the human pressure distributions on width very well.

Measurements were repeated five times in the normal position, and with five different foot positions for the adult surrogates. The measurement precision, as estimated by the standard deviation of parameter values, was consistently below 10 percent of the mean parameter values. For comparison, the difference in target values for width parameters between the six-year-old and small-adult-female categories is about 30 percent of the mean for the two groups. Positioning precision was excellent for the child surrogates, but the variance in the fore-aft position of the adult surrogates on the seat was larger than expected. Although the adult surrogates are inherently more difficult to position than the child surrogates, the repeatability might be improved by additional refinement of the installation procedures. However, the installation variability is much smaller than the positional variance for similarly sized humans, and did not appear to have a substantial effect on the variance of the pressure distribution parameters.

The two adult surrogates, while similar anthropometrically, were tested with two different shoe styles, one having a nearly flat heel and one having a heel height of about 25 mm. The effects of this small difference on the pressure distribution parameters demonstrates the potential sensitivity of seat-based occupant classification systems to subtle changes in occupant behavior. The higher heel was associated with smaller contact area on the seat and larger vertical foot support force. In the knees-up condition, the foot support force was almost twice as great for the Hybrid III as for the OCATD, although this may have been due in part to the difference in hip joint stiffness.

The data from this study suggest that the pressure distributions produced by the Hybrid III dummies are generally within the range of variability expected for humans of similar size. The OCATD performance is slightly better, particularly for the six-year-old, and the advantages of the OCATD are probably greater on firmer seats. This study reinforces the observations from the previous study concerning the effects of posture on pressure distribution parameters. Even in the normal posture, the foot position of the adult surrogates strongly affects the weight borne by the seat and the area-related pressure distribution parameters.

The buttock contours of the OCATDs produce seat surface pressure contours that are visually a better match to the human pressure distributions than those produced by the Hybrid IIIs, but much of the correspondence is not meaningful for occupant classification. For example, the most salient feature of a human pressure distribution pattern is usually the two ischial tuberosity peaks in the buttock area. However, the location and spacing of these peaks was not found to be useful for occupant classification in data from human subjects. Hence, while the contouring of the OCATDs makes the pressure distributions appear more realistic, the width and area of the pressure distributions are more important for occupant classifications. On these parameters, the SFH3 pressure distribution is approximately as accurate as the OCATD5. The 6YOH3 produces pressure distributions that are slightly too narrow, and hence the OCATD6, which has a very accurate pressure distribution width, is more representative of six-year-old children.

The only parameter on which the Hybrid IIIs differed substantially from the OCATDs (and the human targets) was pseudoweight. Pseudoweight is the product of the sensor area and pressure and is a rough measure of the weight borne by the seat cushion. Pseudoweight is difficult to interpret because it is affected by the shape of the contact surface. The pressure distribution measurement system measures, in effect, the aggregate force perpendicular to the surface of the measurement pad. However, the pads are deformed as the surrogate or occupant deflects the seat cushion, so that the perpendicular forces are not vertical. The more angular buttock shape of the Hybrid III dummies may have accounted for the difference in psuedoweight.

One important advantage of the OCATDs over the Hybrid IIIs is that they are easier to position and are capable of a wider range of postures. While the certification test procedures do not require a large range of postures for airbag suppression testing, developmental tests of airbag systems require a much larger range of surrogate postures. For these tests, the posturing advantages of the OCATDs will be valuable. The OCATDs also have more realistic body contours outside of the seat contact areas than the Hybrid IIIs, which may be important for use with sensing systems that are not seat-based.

Only one of each type of surrogate was used in this testing. It is possible, though unlikely, that differences within surrogate category would affect the findings. As with any study of this type, the applicability of the findings is limited to the types of seats and postures used. The characteristics of the pressure-distribution measurement system may also have influenced the results. In particular, a system with lower resolution, such as most of those that have been proposed for use in production seats, may show larger or smaller differences between the OCATDs and Hybrid IIIs.

5.0 REFERENCES

Reed, M.P., Ebert, S.M., Lehto, M.M., and Schneider, L.W. (2000). Development of anthropometric and performance standards for Occupant Classification Anthropomorphic Test Devices (OCATD). Technical Report UMTRI-2000-38. University of Michigan Transportation Research Institute, Ann Arbor, MI.

Reed, M.P., Lehto, M.M., Schneider, L.W., Moss, S., Nghi, T. (2001). Development of anthropometric specifications for the six-year-old OCATD. Technical Paper 2001-01-1057. Warrendale, PA: Society of Automotive Engineers, Inc.